

Numerical simulations of viscoelastic flow around sharp corners

Manuel A. Alves^{a,*}, Paulo J. Oliveira^b, Fernando T. Pinho^c

^a Departamento de Engenharia Química, CEFT, Faculdade de Engenharia da Universidade do Porto, Rua Roberto Frias, 4200-465 Porto, Portugal

^b Departamento de Engenharia Electromecânica, Universidade da Beira Interior, 6200 Covilhã, Portugal

^c Centro de Estudos de Fenómenos de Transporte, DEMEGI, Faculdade de Engenharia da Universidade do Porto, Rua Roberto Frias, 4200-465 Porto, Portugal

Abstract

A finite volume numerical method is applied to the simulation of the flow of a viscoelastic fluid around a sharp corner. The fluid obeys the upper convected Maxwell model and the numerical method is second-order accurate in space. Results show that, near a sharp 270-degree corner, velocity behaves asymptotically as $r^{5/9}$ and stress as $r^{-2/3}$ where r is the radial distance from the corner, thus confirming Hinch's theory. These exponents are seen not to depend on the local polar angle from the corner, but some weak dependency is found on the Deborah number of the flow.

Keywords: Numerical simulations; Finite-volume method; Viscoelastic; Corner; Asymptotic behaviour; Singular point

1. Introduction

Numerical simulations of flow problems involving non-Newtonian fluids are difficult because of two orders of reasons. The first is that most of those fluids exhibit elastic behaviour and consequently the stress field required to determine the kinematics of the motion obey its own constitutive equations, which must be solved in conjunction with the mass and momentum equations. Hence, the mathematical problem is increased from the usual set of four differential equations, for the three velocity components and pressure, by six additional differential equations for the evolution of the six stress components. The second reason for greater difficulty is that for viscoelastic fluids the kinematics near singular points, which invariably arise due to abrupt changes in the geometry enveloping the flow domain, presents a much stronger degree of singularity compared with Newtonian fluids. By this we mean that if stresses behave as $\tau \sim f(\theta)r^{-\alpha}$, where r is the radial distance from the singular point and α is the exponent measuring the rate of growth, then α tends to be larger for the viscoelastic fluids. Near abrupt corners this question is well understood for Newtonian fluids [2] but this is not the case for viscoelastic non-Newtonian fluids for which a few theo-

ries are available [1,3], but where the assumptions invoked have had scarce confirmation from numerical simulations [4,5]. The actuality of this problem is demonstrated by very recent papers (see e.g. Tanner et al. [6]).

In this work the finite volume method (FVM) developed by the authors [7] is applied to scrutinise the stress and velocity behaviour near the 270° sharp corner in a 4:1 planar contraction flow. The fluid follows the upper convected Maxwell model (UCM). We start with an outline of the FV procedure for viscoelastic fluid motion and then we analyse the resulting behaviour near the corner.

2. Governing equations and numerical method

The analysis of the flow of a UCM fluid around a sharp corner requires solution of equations expressing mass conservation of an incompressible fluid,

$$\nabla \cdot \mathbf{u} = 0 \quad (1)$$

momentum conservation in the absence of body forces,

$$\rho \frac{D\mathbf{u}}{Dt} = -\nabla p + \nabla \cdot \boldsymbol{\tau} \quad (2)$$

and a constitutive equation for the extra stress tensor $\boldsymbol{\tau}$:

$$\boldsymbol{\tau} + \lambda \frac{D\boldsymbol{\tau}}{Dt} = 2\eta \mathbf{D} + \lambda (\boldsymbol{\tau} \cdot \nabla \mathbf{u} + \nabla \mathbf{u}^T \cdot \boldsymbol{\tau}) \quad (3)$$

* Corresponding author. Tel.: +351 (22) 508-1680; Fax: +351 (22) 508-1440; E-mail: mmalves@fe.up.pt

The viscosity coefficient η and the relaxation time λ in the UCM Eq. (3) are constant. In our problem the required boundary conditions are no-slip at solid walls ($\mathbf{u} = \mathbf{0}$, $\tau_{nn} = 0$, $\tau_{n\tau} = 2\eta\lambda\dot{\gamma}^2$, $\tau_{\tau\tau} = \eta\dot{\gamma}$, with $\dot{\gamma} = du_\tau/dn$), imposed fully developed profiles at inlet, parabolic conditions at outlet for both the velocity and stress fields, and symmetry conditions at the centerline ($y = 0$).

Following standard finite volume techniques in non-staggered meshes, the momentum equations are integrated over a control volume (CV) yielding algebraic equations of the form:

$$a_P \mathbf{u}_P = \sum_F a_F \mathbf{u}_F + \mathbf{S}_u \quad (4)$$

where index P denotes any CV, index F denotes surrounding CVs, a_P and a_F are coefficients composed by convective and diffusive contributions, and \mathbf{S}_u is a source term. Eq. (4) is implicitly solved for \mathbf{u} by means of a bi-conjugate gradient method. The resulting velocity field does not satisfy continuity, which must then be enforced by application of velocity and pressure corrections, with these obtained from a pressure correction Poisson equation as explained in [7].

The constitutive equation is discretised in a way similar to that of the momentum equation resulting in:

$$a_P^\tau \tau_P = \sum_F a_F^\tau \tau_F + \mathbf{S}_\tau \quad (5)$$

in which the source term, from Eq. (3), is:

$$\mathbf{S}_\tau = \sum_l^3 (\mathbf{b}_l [\Delta \mathbf{u}]_l + [\Delta \mathbf{u}]_l \mathbf{b}_l) + \frac{\lambda V}{\delta t} \tau^n + \mathbf{S}_{\tau\text{-HOS}} \quad (6)$$

where V is the volume of a CV, δt is the time step, HOS denotes additional source terms from higher-order schemes [5], $[\Delta \mathbf{u}]_l$ are velocity differences along direction l ($l = 1, 2, 3$), and $\mathbf{b}_l = \eta \mathbf{B}_l + \lambda \mathbf{B}_l \cdot \tau$ (\mathbf{B}_l are vector areas of CV surfaces pointing along direction l). A key point in the algorithm is the determination of stresses at CV faces, required by the term $\nabla \cdot \tau$ in Eq. (2), and the

way to do this is detailed in [7]. It is also important to emphasize that, because of the hyperbolic nature of Eq. (3), the convective term must be discretised with a differencing scheme generating small amounts of numerical diffusion. We have used high-resolution schemes [5] that ensure stability and second order accuracy in space.

3. Results

The flow configuration is seen in Fig. 1 which also presents the predicted streamlines for one of the flow conditions. Our objective is to study the conditions near the sharp corner located at $x = 0$ and $y = H$, where H is the half-width of the small channel in which the average cross-section velocity is U . The relevant dimensionless groups are the Reynolds number, $Re = \rho U H / \eta$, which is always very small ($= 0.01$), and the Deborah number, $De = \lambda U / H$, which is a measure of elastic effects. Streamlines in Fig. 1 are for $De = 1$ and one can already see evidence of elastic effects by the very small lip vortex established near the corner (singularity). This rather small lip vortex is not detrimental to the validity of the theory developed by Hinch [1] as evidenced by the asymptotic plots of Figs. 3 and 4. In Fig. 2 we show the results for the Newtonian case and demonstrate a close agreement with

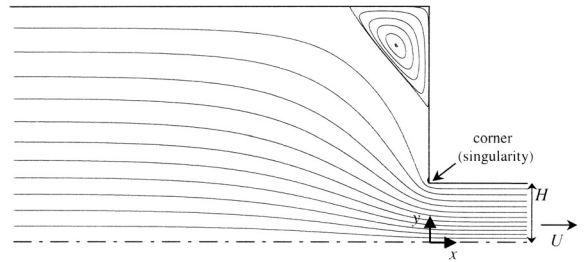


Fig. 1. Configuration of the contraction flow and streamlines at $De = 1$.

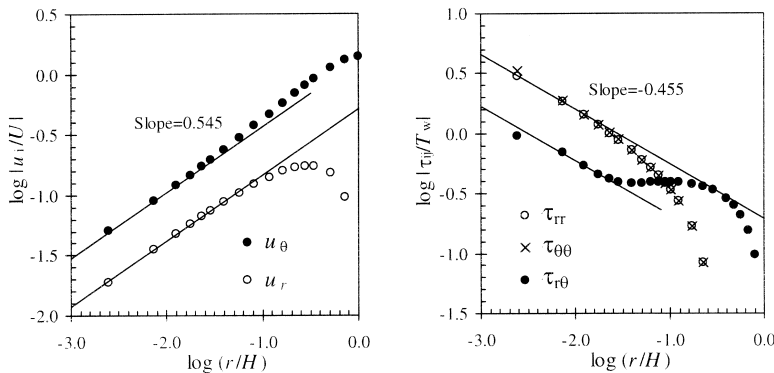


Fig. 2. Asymptotic behaviour near the corner for the Newtonian case

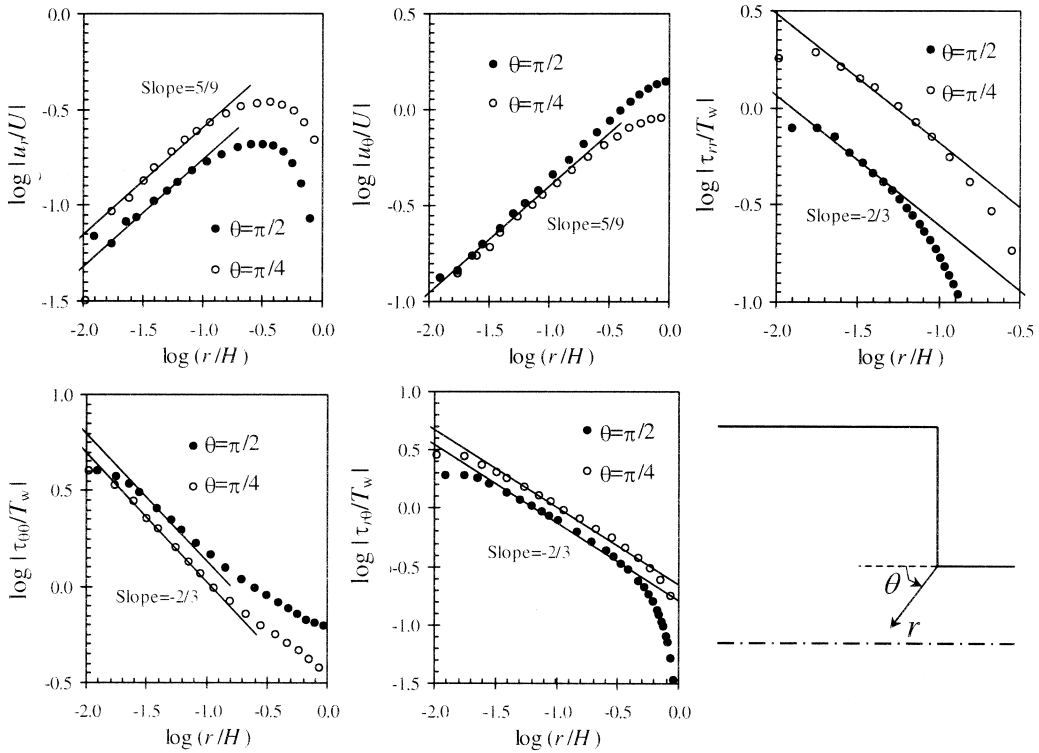


Fig. 3. Asymptotic behaviour near the corner for the UCM case at $De = 1$ for two polar angles ($T_w = 3\eta U/H$).

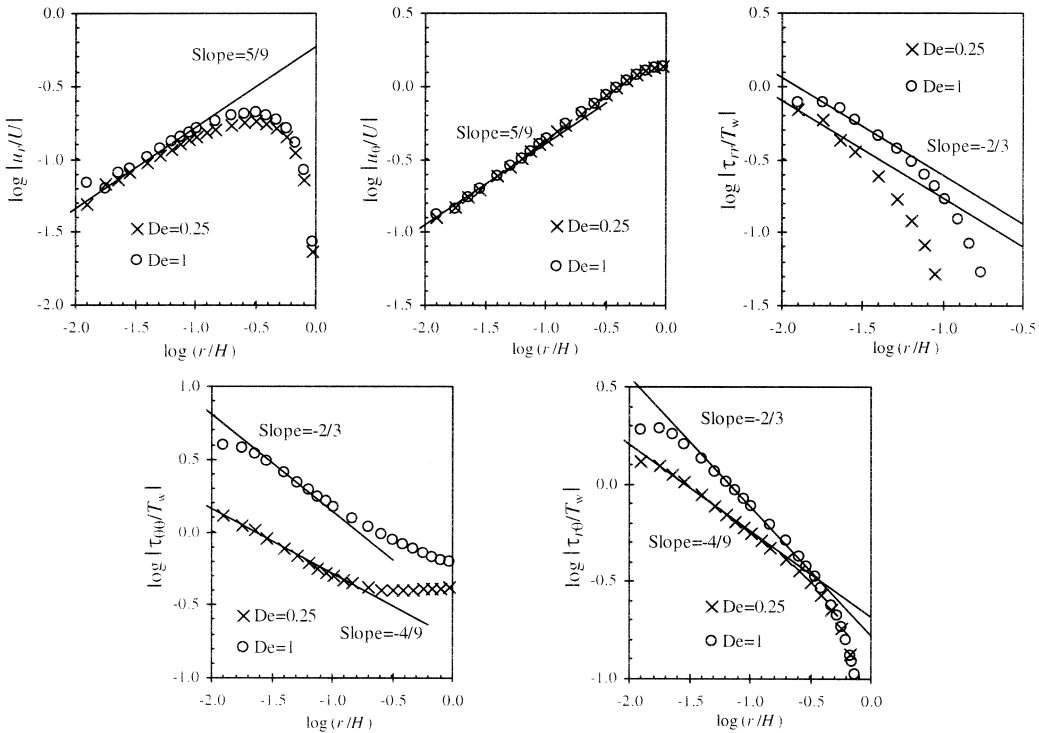


Fig. 4. Effect of the Deborah number on the asymptotic behaviour.

the theory of Dean and Montagnon [2], with velocities decreasing as $r^{+0.545}$ and stresses increasing (to infinity) as $r^{-0.455}$. The fact that stresses are singular does not seem to impede or deteriorate iterative convergence of the numerical method and, furthermore, the accuracy, as compared with the theoretical results, seems good and devoid of oscillations.

For the viscoelastic cases (Figs. 3 and 4) some numerical oscillations are present in the first few nodes very close to the wall, due to the steep gradients and inaccuracies introduced by the boundary conditions. However, power-law asymptotic profiles are clearly established beyond those first couple of nodes and, in Fig. 3, we compare the predictions with the theoretical slopes of Hinch for the 'core region' and we investigate the possible effect of the angle θ ($\theta = \pi/2$ corresponds to the line $x = 0$ in Fig. 1). The similarity solution of Hinch is of the form $\tau \approx Q f(\theta) r^{-\alpha}$ (with $\alpha = 2/3$) and so, in a log-log plot, the effect of varying θ is to shift up or down the straight lines but keeping the same slope. As seen in Fig. 3, the numerical predictions at $De = 1$ confirm the $-2/3$ slope for stresses and $+5/9$ for velocities, as well as the separable similarity solution.

In Fig. 4 we investigate possible Deborah number effects by comparing predictions at $De = 0.25$ and 1. Hinch analysis suggests that such De effects should be embodied in the amplitude Q which is determined by upstream conditions away from the corner. This supposition is confirmed by the numerical predictions for the velocity components (the slope $5/9$ is maintained) and the normal stress (same slope $-2/3$). However, the other normal stress $\tau_{\theta\theta}$ and the shear stress $\tau_{r\theta}$ seem to have a weaker singularity at

the lower De . In fact, the asymptotic variation for those stress components at $De = 0.25$ is seen in Fig. 4 to follow very well the slope $-4/9$ which was derived by Hinch as being valid for the solvent stress in the core region. We recall that Hinch's solution was obtained for the Oldroyd-B fluid which possesses, in addition to a Maxwell stress, a Newtonian solvent viscosity η_N (i.e. $\tau_{\text{Old-B}} = \tau + 2\eta_N \mathbf{D}$). The UCM fluid does not have a solvent viscosity but it is always possible to decompose its stress in an elastic part plus a Newtonian-like part (as $\tau = \tau_E + 2\eta \mathbf{D}$). We can then only speculate that, as De is reduced (as in Fig. 4), the assumption made by Hinch that the elastic stress dominates the Newtonian stress becomes less valid and, below a certain De , the stress behaviour will tend to follow the $-4/9$ line of the 'solvent' stress.

References

- [1] Hinch EJ. *J Non-Newt Fluid Mech* 1993;50:161–171.
- [2] Dean WR, Montagnon PE. *Proc Cambr Philos Soc* 1949;45:389–394.
- [3] Renardy M. *J Non-Newt Fluid Mech* 1993;50:127–134.
- [4] Xue S-C, Phan-Thien N, Tanner RI. *J Non-Newt Fluid Mech* 1998;74:195–245.
- [5] Alves MA, Pinho FT, Oliveira PJ. *J Non-Newt Fluid Mech* 2000;93:287–314.
- [6] Tanner RI, Jabbarzadeh A, Xue S-C. *Proc XIIIth Int Congress on Rheology*, Cambridge 2000;2:181–183.
- [7] Oliveira PJ, Pinho FT, Pinto GA. *J Non-Newt Fluid Mech* 1998;78:1–43.